

## Research Note

### An Analysis of the Barr Effect

M. G. Fracastoro

Astronomical Observatory of Torino, I-10025 Pino Torinese, Italy

Received February 26, 1979

**Summary.** From the data contained in the VII Catalogue of the orbital elements of Spectroscopic Binary Systems recently published by Batten et al., some aspects of the Barr effect are examined. In particular, the values of eccentricity  $e$  and longitude of periastron  $\omega$  in terms of the orbital period  $P$  have been considered. The percentage of spurious eccentricities is tentatively evaluated. The non uniform distribution of the  $\omega$ -values partly remains also for long period systems and even when only large eccentricities are taken into account.

**Key words:** spectroscopic orbits – longitude of periastron – eccentricity

The distribution of the periastron angles  $\omega$  among close binaries (Barr effect) has been examined and discussed by several authors. Among other topics, this distribution was examined by the present writer in a paper (Fracastoro, 1978) which was prepared shortly before the publication of Batten's VII Catalogue of orbital elements of Spectroscopic Binary Systems (Batten, 1978). Therefore, it appeared worthwhile to reexamine the distribution of the  $\omega$ 's resulting from this improved and enlarged Catalogue.

All systems have been arranged according to their period  $P$  for intervals  $\Delta \log P = 0.2$ , with reference to  $\log P = 0.0$  (even intervals) or to  $\log P = 0.1$  (odd intervals). The same has been done for those spectroscopic binaries which are also observed photometrically as eclipsing binaries. The resulting distribution is shown in Table 1. See also Figs. 1 and 2.

The fraction of spectroscopic binaries and eclipsing systems showing circular orbits decreases steadily with increasing period, as expected. However, this percentage is considerably smaller for the generality of spectroscopic binaries than for eclipsing systems, where a significant number of eccentricities is forced to zero, because they are disproved by the photometric curve (see Fig. 3). For instance, around  $P = 10^d$ , we have 96 spectroscopic binaries, and 76 among them (79%) show eccentric orbits. Among these 96 systems, 22 are eclipsing binaries, and only 11 among them show eccentricities (50%). Consequently, of the 74 not eclipsing spectroscopic systems, 65 show eccentric orbits (88%), instead of 37. In conclusion, eccentricities should be spurious for 28 systems, most of them being probably of modest amount ( $e \leq 0.2$ ).

The general trend of this fraction of circular orbits versus increasing period, both for spectroscopic binaries and eclipsing systems is shown in Fig. 3, where the area between the two smoothed curves should correspond to spurious eccentricities.

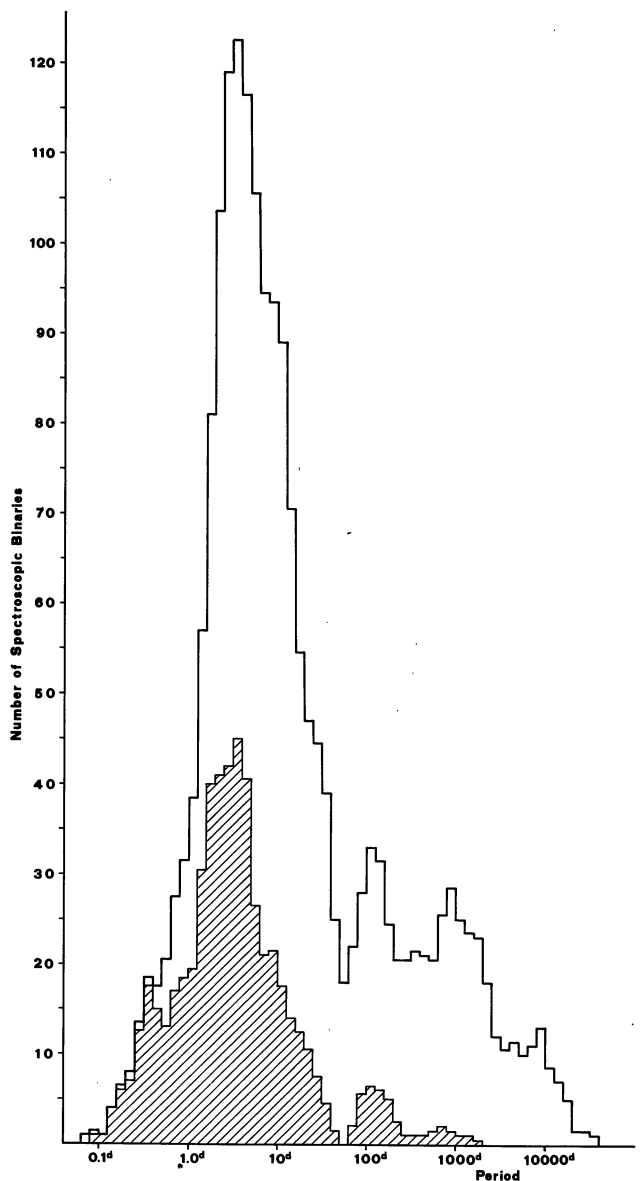


**Fig. 1.** All spectroscopic binaries arranged in terms of increasing period  $P$ , for intervals  $\Delta \log P = 0.2$ . The double plot results from even and odd intervals. The shaded area contains the systems showing circular orbits. All data are taken from VII Catalogue of Orbital Elements of Spectroscopic Binary Systems issued by Batten et al.

Table 1

| Number of spectroscopic binaries |     |                  |     | Number of eclipsing binaries |     |                  |     | Period (days) |
|----------------------------------|-----|------------------|-----|------------------------------|-----|------------------|-----|---------------|
| All interval                     |     | $e > 0$ interval |     | All interval                 |     | $e > 0$ interval |     |               |
| even                             | odd | even             | odd | even                         | odd | even             | odd |               |
|                                  | 1   | 1                |     | 1                            | 1   |                  |     | 0.1           |
| 1                                | 0   | 1                | 0   | 1                            | 0   | 1                | 0   |               |
| 2                                | 6   | 0                | 0   | 2                            | 6   | 0                | 0   |               |
| 7                                | 9   | 1                | 1   | 6                            | 7   | 1                | 1   |               |
| 18                               | 19  | 1                | 1   | 15                           | 17  | 0                | 0   |               |
| 16                               | 25  | 4                | 11  | 13                           | 21  | 2                | 9   |               |
| 30                               | 33  | 10               | 16  | 26                           | 19  | 8                | 4   |               |
| 44                               | 70  | 22               | 31  | 21                           | 39  | 7                | 16  |               |
| 92                               | 115 | 51               | 74  | 46                           | 44  | 23               | 22  |               |
| 123                              | 120 | 80               | 73  | 48                           | 45  | 26               | 21  |               |
| 113                              | 98  | 79               | 79  | 33                           | 23  | 15               | 15  |               |
| 91                               | 96  | 68               | 76  | 24                           | 22  | 13               | 11  |               |
| 82                               | 59  | 67               | 46  | 19                           | 11  | 10               | 5   |               |
| 50                               | 44  | 38               | 35  | 8                            | 5   | 3                | 1   |               |
| 45                               | 33  | 39               | 30  | 5                            | 4   | 3                | 3   |               |
| 17                               | 17  | 17               |     | 0                            | 0   | 0                | 0   |               |
| 25                               | 31  | 21               | 24  | 2                            | 2   | 0                | 0   |               |
| 35                               | 28  | 29               | 22  | 0                            | 2   | 0                | 1   |               |
| 21                               | 20  | 17               | 19  | 3                            | 2   | 2                | 2   |               |
| 21                               | 22  | 20               | 21  | 2                            | 1   | 2                | 1   |               |
| 20                               | 21  | 19               | 19  | 1                            | 2   | 1                | 1   |               |
| 30                               | 27  | 28               | 26  | 3                            | 3   | 2                | 2   |               |
| 23                               | 24  | 22               | 23  | 2                            | 1   | 2                | 1   |               |
| 22                               | 14  | 22               | 14  | 0                            | 0   | 0                | 0   |               |
| 10                               | 11  | 10               | 11  | 2                            | 2   | 2                | 2   |               |
| 12                               | 8   | 12               | 8   | 0                            | 1   | 0                | 1   |               |
| 14                               | 14  | 14               |     | 3                            | 3   | 3                |     |               |
|                                  | 12  | 12               |     | 2                            | 2   | 2                | 2   |               |

| Number of spectroscopic binaries |     |                  |     | Number of eclipsing binaries |     |                  |     | Period (days) |
|----------------------------------|-----|------------------|-----|------------------------------|-----|------------------|-----|---------------|
| All interval                     |     | $e > 0$ interval |     | All interval                 |     | $e > 0$ interval |     |               |
| even                             | odd | even             | odd | even                         | odd | even             | odd |               |
| 5                                |     | 5                |     |                              |     |                  |     |               |
|                                  | 9   |                  | 9   |                              |     |                  |     |               |
| 1                                |     | 1                |     |                              |     |                  |     |               |
|                                  | 2   |                  | 2   |                              |     |                  |     |               |
| 1                                |     | 1                |     |                              |     |                  |     |               |
|                                  | 1   |                  | 1   |                              |     |                  |     |               |

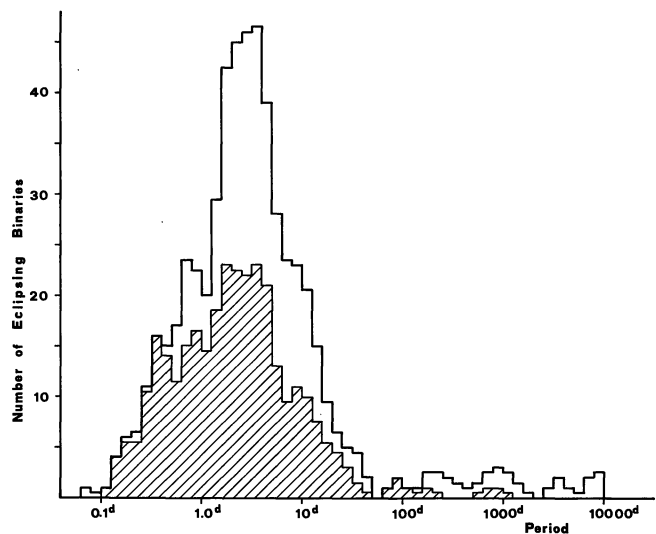


Fig. 2. The same distribution as Fig. 1, limited to eclipsing binaries. The scale is the same as in Fig. 1. The shaded area is referred again to circular orbits

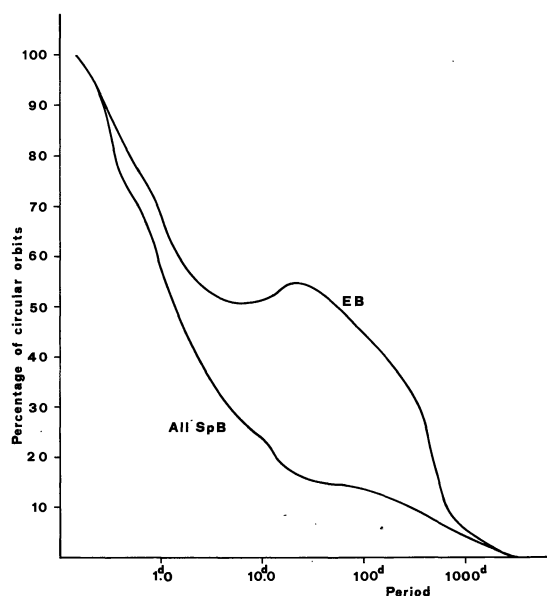
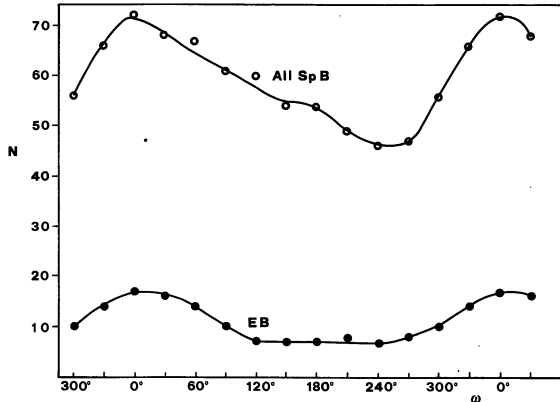


Fig. 3. The percentage of circular orbits with increasing period among all spectroscopic binaries and eclipsing systems

**Table 2**

|                            | $\omega$                          | 345 | 15               | 45               | 75               | 105 | 135 | 165 | 195              | 225             | 255             | 285              | 315 | 345 |
|----------------------------|-----------------------------------|-----|------------------|------------------|------------------|-----|-----|-----|------------------|-----------------|-----------------|------------------|-----|-----|
| All spectroscopic binaries | Unambiguous                       | 72  | 65               | 48               | 72               | 48  | 47  | 50  | 48               | 31              | 43              | 50               | 61  |     |
|                            | Ambiguous (weight $\frac{1}{2}$ ) | 14  | 16               | 8                | 11               | 14  | 4   | 14  | 15               | 8               | 12              | 15               | 4   |     |
|                            | Total                             | 79  | 73               | 52               | 77 $\frac{1}{2}$ | 55  | 49  | 57  | 55 $\frac{1}{2}$ | 35              | 49              | 57 $\frac{1}{2}$ | 63  |     |
| Eclipsing binaries         | Unambiguous                       | 16  | 20               | 10               | 11               | 6   | 4   | 7   | 8                | 5               | 7               | 8                | 13  |     |
|                            | Ambiguous (weight $\frac{1}{2}$ ) | 2   | 1                | 1                | 0                | 4   | 2   | 2   | 1                | 3               | 1               | 3                | 2   |     |
|                            | Total                             | 17  | 20 $\frac{1}{2}$ | 10 $\frac{1}{2}$ | 11               | 8   | 5   | 8   | 8 $\frac{1}{2}$  | 6 $\frac{1}{2}$ | 7 $\frac{1}{2}$ | 9 $\frac{1}{2}$  | 14  |     |



**Fig. 4.** Distribution of the periastron angles  $\omega$  for all spectroscopic binaries and for eclipsing binaries

**Table 3**

| No. | Interval  | $\omega_{max}$ | $\omega_{min}$ | $\frac{N_{min}}{N_{max}}$ |
|-----|-----------|----------------|----------------|---------------------------|
| 31  | 1.26–1.99 | 100°           | 320°           | 4.0                       |
| 75  | 1.99–3.16 | 75             | 270            | 2.7                       |
| 73  | 3.16–5.01 | 45             | 195            | 2.4                       |
| 79  | 5.01–7.95 | 15             | 225            | 1.6                       |
| 76  | 7.95–12.6 | ...            | ...            | (1.2)                     |
| 48  | 12.6–19.9 | ...            | ...            | (1.3)                     |
| 35  | 19.9–31.6 | (345)          | (250)          | (2.2)                     |
| 30  | 31.6–50.1 | 315            | 105            | 3.0                       |
| 19  | 50.1–79.5 | 345            | 165            | 5.0                       |
| 24  | 79.5–126  | ( 50)          | (220)          | (1.6)                     |
| 22  | 126–199   | 10             | 125            | 2.1                       |
| 19  | 199–316   | 340            | 75             | 3.3                       |
| 20  | 316–501   | 45             | 135            | 3.0                       |

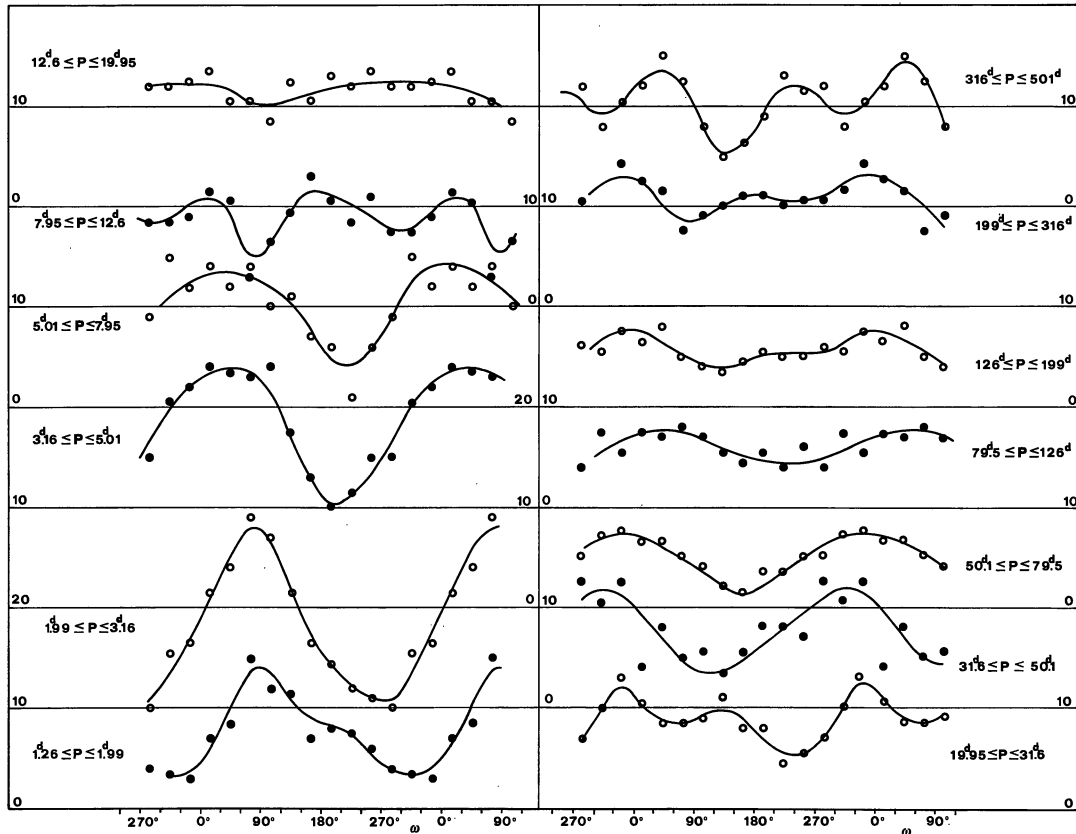


**Fig. 5.** The Barr effect analysed for various intervals of increasing period

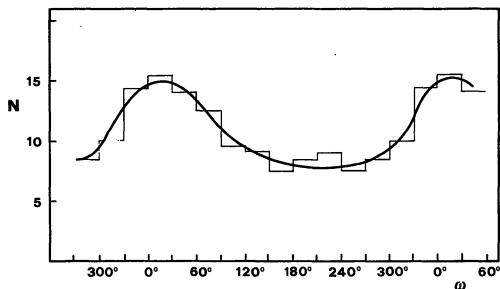


Fig. 6. Distribution of the periastron angles for spectroscopic binaries having large values of eccentricity ( $e \geq 0.60$ )

The histogram of all  $\omega$ 's reported in Catalogue VII shows that their anomalous distribution remains (see Table 2 and Fig. 4), with a maximum frequency around  $0^\circ$  and a flat minimum around  $\omega = 250^\circ$ . The trend is much less pronounced, instead, when only eclipsing binaries are considered.

In our previous paper (Fracastoro, 1978) it was pointed out that, if we compare a sinusoidal velocity curve with that resulting for  $\omega = 0^\circ$  and  $e = 0.2$ , the differences in terms of radial velocity speak in favour of gas streams flowing from the cooler evolved component to the hotter one. This is actually the most common process occurring in semi-detached systems. The velocity curve resulting from  $\omega = 180^\circ$  ( $e = 0.2$  again) suggests the opposite phenomenon, which is certainly less common.

An inspection of the Barr effect for the various groups of spectroscopic binaries, according to the assumed  $\Delta \log P$ , may bring some contribution to the interpretation of the effect itself. Starting from the interval  $1^d26 \leq P \leq 1^d99$  (for shorter periods the

orbits are almost all circular), we observe (see Fig. 5) a definite trend, which remains for the two subsequent intervals, up to  $P = 5^d01$ . For still longer periods, the Barr effect seems to disappear, but it becomes evident again from  $P = 50^d1$  up to  $79^d5$ . Table 3 summarizes the number of systems considered within each interval, the range of period, the  $\omega$ -value most frequently recorded and that corresponding to a minimum occurrence of cases. Finally, it is reported the ratio between the maximum and the minimum number, as an indication of the reliability of the unequal distribution. All curves have been smoothed, including three counts instead of one, for each interval of  $\omega$  ( $30^\circ$ ).

Finally, we have considered systems having very strong eccentricity ( $e \geq 0.60$ ), regardless of their period, in order to eliminate all those small values of  $e$  which might be responsible for the Barr effect, being due to a biased interpretation of the velocity curves. As a matter of fact, these systems with large eccentricity show clearly a marked Barr effect (Fig. 6), with a maximum frequency for  $\omega = 20^\circ$  and a minimum occurrence for  $\omega$ 's around  $225^\circ$ . Consequently, we are forced to admit that either the gas streams are so strong that the velocity curves can be profoundly altered, or there is a tendency to find  $\omega$ -values close to  $0^\circ$  during the reduction phase of the velocity curves.

#### References

- Batten, A.H., Fletcher, J.M., Mann, P.J.: 1978, Publications of the Dominion Astrophysical Observatory, Victoria B.C. Volume XV, No. 5
- Fracastoro, M.G.: 1978, Coloquio sobre "Sistemas binarios cerados", S. Paulo, Brasil, 1978